ISBN: 978-3-95450-253-0 ISSN: 2673-5571 doi:10.18429/JACoW-HB2023-FRC1I3

DEVICES FOR HIGH-EFFICIENCY SLOW EXTRACTION AT J-PARC MAIN RING

R. Muto*, T. Kimura, S. Murasugi, K. Numai, K. Okamura, Y. Shirakabe, M. Tomizawa, E. Yanaoka
High Energy Accelerator Research Organization (KEK), Ibaraki, Japan
A. Matsumura, NAT corporation, Ibaraki, Japan

Abstract

J-PARC Main Ring (MR) is a synchrotron that accelerates protons up to 30 GeV and supplies them to the Neutrino Experimental Facility and the Hadron Experimental Facility (HEF). Beam extraction from MR to HEF is performed by slow extraction using third-order resonance. In the slow extraction, electrostatic septa (ESS) are used to scrape off the beam, and it is crucial to reduce the beam loss at the septum electrode of the ESS to supply a high-intensity beam. So far, we have achieved a slow extraction efficiency of 99.5 % by developing an ESS with a thin septum electrode and tuning the orbit bump to reduce the angular spread of the proton beam at the ESS. In addition, a collimator is installed downstream of the ESS to absorb particles scattered by the septum electrode, thereby reducing the activation of the components downstream. In order to achieve further reduction of the beam loss, we are considering installing beam diffusers or bent silicon crystals upstream of the ESS.

INTRODUCTION

At the J-PARC Main Ring, proton beams accelerated up to 30 GeV are extracted towards the Neutrino Experimental Facility or Hadron Experimental Facility (HEF) to promote particle and nuclear physics experiments [1]. Beam extraction to the HEF is performed by slow extraction using the third-order resonance of betatron oscillations. By 2021, we achieved user operation with a beam power of approximately 64 kW with an extraction efficiency of about 99.5 %. In this slow extraction, a device called an electrostatic septum (ESS) [2] is used to extract the beam by scraping off the particles with increased betatron amplitude due to third-order resonance. A high electric field between the septum electrode and the cathode of the ESS achieves beam scraping. Since inserting a septum electrode into the beam is necessary, large beam losses due to particles colliding with the septum electrode are inevitable. Therefore, major issues are reducing beam loss at the septum electrode and localizing peripheral device activation by scattered particles. In this paper, we will briefly explain the slow extraction method at J-PARC Main Ring and then describe the devices and their features.

SLOW EXTRACTION AT J-PARC MAIN RING

Table 1 shows the basic parameters for the slow extraction of the J-PARC Main Ring. The injection energy of the proton beam is 3 GeV, and the ESS is installed in the upstream part of the slow extraction straight section at a transverse position where the septum electrode does not interfere with the injection beam. As the beam emittance decreases with acceleration from 3 GeV to 30 GeV, a orbit bump is created in the slow extraction straight section, bringing the closed orbit of the beam closer to the high electric field region created by the septum electrode and the cathode of the ESS. The electric field is generated between 60 mm and 85 mm in the horizontal position, and the center of the orbit bump is located at 35 mm, here the origin is the center of the circulating beam. Next, by approaching the horizontal betatron tune to 22.333 from below, we will reduce the area of the stable region in the phase space. The particles return to approximately the same position every three turns. However, the amplitude of the particles that protrude into the unstable region gradually increases along the separatrix that separates the stable and unstable regions. Figure 1 shows the movement of particles with various amplitudes in horizontal normalized phase space when the horizontal betatron tune is kept constant.

Table 1: Basic Parameters for the Slow Extraction at J-PARC MR

Parameter	Value
Particle	Proton
Circumference	1567.5 m
Injection energy	3 GeV
Extraction energy	30 GeV
Horizontal betatron tune	22.31 → 22.333
Vertical betatron tune	20.8
Repetition	5.2 s
Spill length	~ 2 s

The high electric field between the septum electrode and the cathode kicks particles that reach the septum electrode of the ESS. In this process, a certain proportion of particles collide with the septum electrode and are scattered at a large angle, resulting in beam loss. Here, step size is defined as the difference between the particle position and that in three turns before. Roughly, the number of beam particles in the ratio of (septum thickness) / (step size at the septum electrode) will collide with the septum electrode. Hence, increasing the step size at the septum electrode and decreasing the septum thickness are important for reducing beam loss. The design value of the step size in J-PARC MR is 20 mm.

Another important point for reducing beam loss is the particles' angular spread at the ESS position. When a par-

* ryotaro.muto@kek.jp

ISBN: 978-3-95450-253-0 ISSN: 2673-5571 doi:10.18429/JACoW-HB2023-FRC1I3

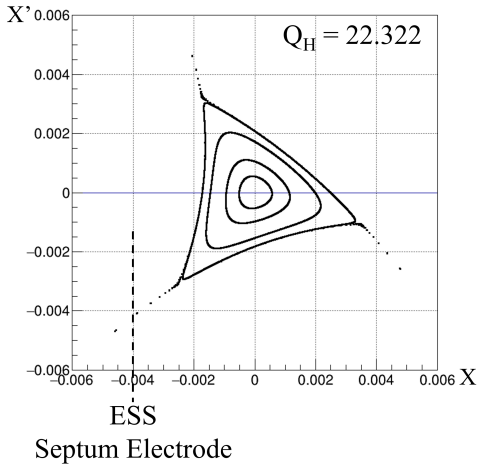

Figure 1: The horizontal motion of particles with various amplitudes in normalized phase space when horizontal betatron tune Q_H is 22.322. The septum electrode of ESS is placed at the position of $X = -0.004$.

ticle protrudes into the unstable region and increases its amplitude, it moves along the separatrix. Suppose this separatrices are in different positions at the beginning and end of extraction. In that case, the angle at which the particles reach the septum electrode will change, increasing beam loss at the septum electrode. Therefore, in the J-PARC MR, the angle of the orbit bump at the ESS entrance is changed in synchronization with the progress of extraction, and the separatrix heading toward the septum electrode of the ESS is controlled so as not to change during extraction. This method is called a dynamic bump scheme [3]. A diagram schematically showing this extraction process is shown in Fig. 2. In addition, the dispersion in the straight section is set to 0, and the chromaticity is also set to approximately 0, so the extraction trajectory is not affected by the particle momentum distribution. Thanks to these beam optics designs and a dynamic bump scheme, the angular spread of

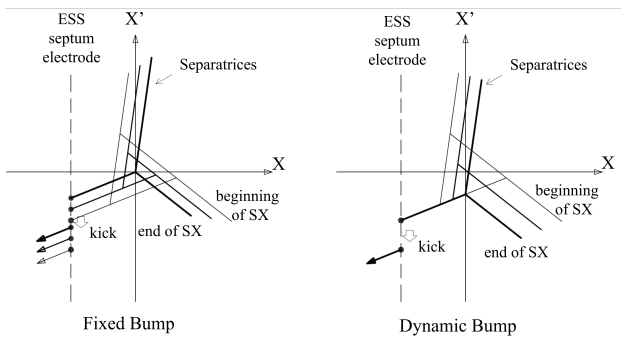

Figure 2: Difference in separatrix changes between fixed bump scheme and dynamic bump scheme. In the dynamic bump scheme, changes in the separatrix during extraction are minimized by changing X' in synchronization with the progress of extraction.

the particles at the position of the septum electrode of the ESS is suppressed to a small value, and beam loss can be reduced. In addition, the beam reduction effect of a beam diffuser or bent crystal, which will be described later, can be improved. In simulations using SAD [4], the angular spread of the particles is estimated to be about 17 µrad.

Particles kicked by the ESS are further kicked by downstream septum magnets [5] and extracted to the HEF. The preferable difference in the horizontal betatron phase between the ESS and the downstream septum magnets is $(90 + 180 \times n)°$, $n = 0, 1, \cdots$, and in the J-PARC Main Ring, it is set to be around 250°, thus the distance between the ESS and the septum magnet is relatively long, approximately 50 m. This makes it possible to place a collimator, which will be described later, between the ESS and the septum magnets. Figure 3 shows the device layout in the slow extraction straight section.

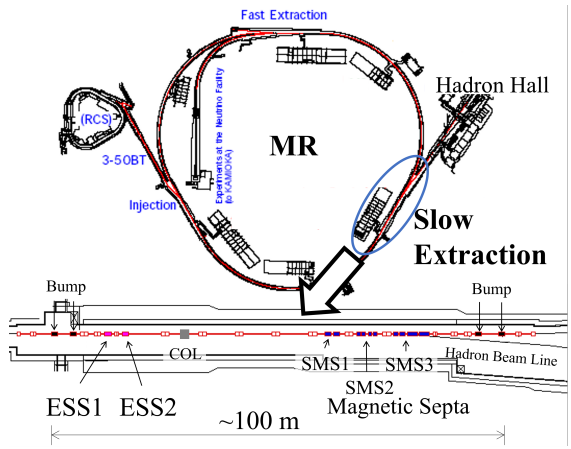

Figure 3: Layout of the devices for the slow extraction in the J-PARC MR straight section.

ELECTROSTATIC SEPTUM (ESS) IN J-PARC MR

Figure 4 shows a photograph of the ESS viewed from the beam entrance direction. Table 2 shows the basic parameters of the ESS. The septum electrode is fabricated by stretching 495 ribbons of 1 mm width at 3 mm intervals on a frame with a length of 1500 mm in the longitudinal direction. A titanium cathode is placed opposite the septum electrode.

Table 2: Basic Parameters of the ESSs at J-PARC MR

Parameter	Value
Voltage / Gap	104.4 kV / 25 mm = 4.2 MV/m
Deflection angle	−0.2 mrad × 2
Longitudinal length	1.5 m
Ribbon thickness	30 µm
Ribbon width	1 mm
Ribbon interval	3 mm
Number of ribbons	495

ISBN: 978-3-95450-253-0 ISSN: 2673-5571 doi:10.18429/JACoW-HB2023-FRC1I3

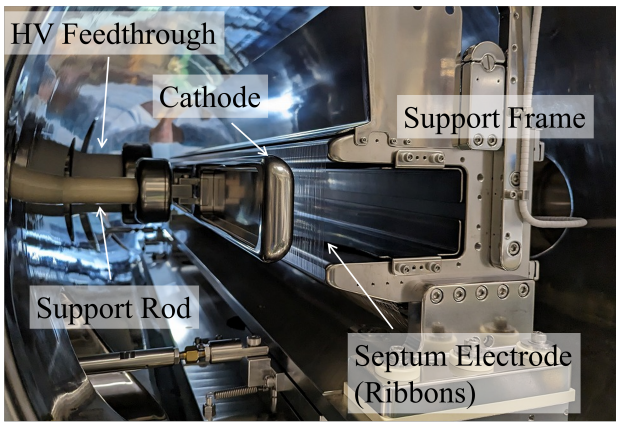

Figure 4: A photograph of the ESS seen from the direction the beam enters.

The distance between the cathode and septum ribbons is 25 mm. The septum ribbons are stretched vertically at 1 kgf to suppress deflection due to the electric field, and we chose a ribbon-like shape to create a thin septum electrode while ensuring the necessary tensile strength. The thickness of the ribbon is approximately 30 µm, manufactured by rolling and annealing and then electrolytically polished. The material is tungsten rhenium alloy, containing 26 % rhenium. A cross-sectional photograph of the ribbon is shown in Fig. 5. After

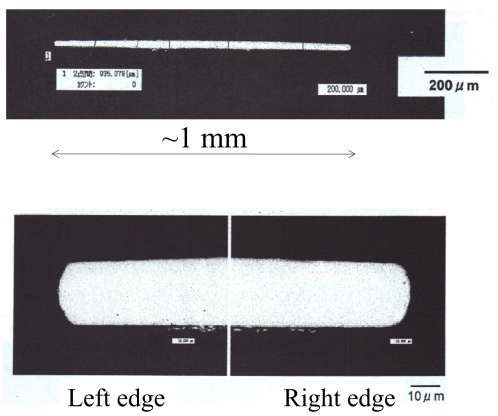

Figure 5: A cross-sectional photograph of the tungsten-rhenium ribbon that makes up the septum electrode of the ESS.

the ribbons are stretched on the frame, their positions are measured using a laser displacement sensor. If the positions of the 500 ribbons are varied or some of them are twisted, the effective thickness of the septum electrode increases, causing beam loss increase. Figure 6 shows an example of position measurement results using a laser displacement sensor. In order to evaluate the effects of the ribbons' positional variations on beam loss, we calculated the energy deposit when the proton beam collides with the septum electrode using FLUKA [6]. The upper panel of Fig. 7 shows the calculation results assuming that ribbons with a thickness of

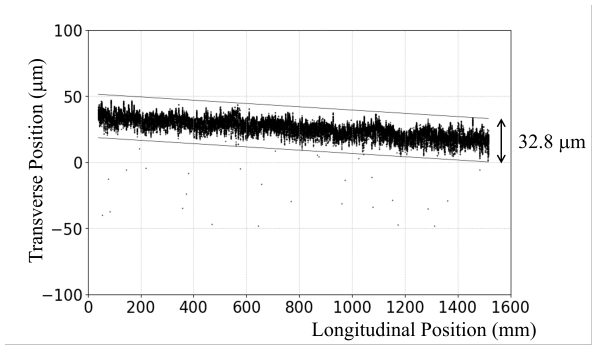

Figure 6: Transverse position of 500 ribbons measured by laser displacement sensor. These are the results for the ESS produced in 2023. The horizontal axis is the longitudinal position. The variation in ribbon position is 33 µm in full width.

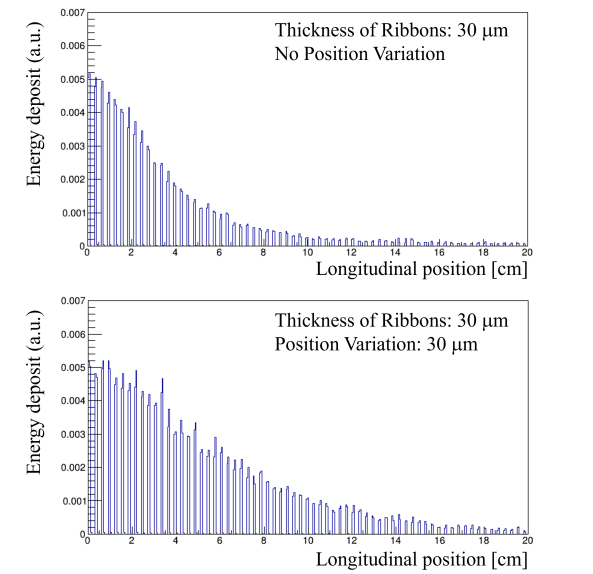

Figure 7: Calculation results using FLUKA for the energy deposit in each ribbon when a 30 GeV proton beam is extracted using ESS. The horizontal axis is the longitudinal position. The upper figure shows the result when the ribbons are lined up ideally without any variation, and the lower figure shows the result when the ribbon positions are varied in a uniform distribution with a width of 30 µm.

30 µm are lined up ideally with no variation in position. It can be seen in the plot that the most upstream ribbon has the largest energy deposit. When charged particles are injected into an object with a large volume, a shower of secondary particles is formed, and the energy deposition is greatest not at the object's surface but at a certain depth determined by the nuclear interaction length. However, this is not the case with the ESS ribbon, because the ribbon is thin and the generated secondary particles escape in transverse direction and do not form a shower. Next, the energy deposit when a uniform random number varies the position of each ribbon is shown in the lower panel of Fig. 7. Here, the total

ISBN: 978-3-95450-253-0 ISSN: 2673-5571 doi:10.18429/JACoW-HB2023-FRC1I3

width of variation was set to 30 µm according to the measurement results in Fig. 6. We can see in this figure that the maximum value of energy deposit in the most upstream ribbon does not change from the no position variation case, but the total energy deposition increases. In other words, even if the total mass of the ribbons is constant, the large variations in the ribbon positions cause the large beam loss. Therefore, it is important to arrange the ribbons with the minimal variation in position. Assuming this energy deposit distribution and cooling only by radiation, the maximum temperature the septum ribbon is estimated to be around 400 °C with 100 kW beam, which is well below the melting point of tungsten-rhenium alloy, about 3000 °C.

The cathode or the ESS is made of pure titanium. High voltage is supplied from outside the chamber via a hermetic feedthrough filled with fluorinert FC-40. The gap between the titanium cathode and the septum electrode is 25 mm, and a voltage of −104.4 kV is applied on the cathode. The kick angle for a 30 GeV beam with a 1.5 m long electric field is 0.2 mrad, and a total kick of 0.4 mrad is given using two electrostatic septa. The horizontal positions and angles of the cathode and the septum electrode can be adjusted independently and remotely. They are controlled by highly radiation-resistant stepper motors, one upstream and one downstream. The position reproducibility is less than 5 µm. The frame for septum ribbons and the vacuum chamber are also made of titanium to reduce the residual radiation dose rate.

BEAM DIFFUSERS AT THE UPSTREAM OF ESS

The user operation has been achieved with a beam power of 64 kW and an extraction efficiency of about 99.5 %. However, the on-contact residual dose rate with 6.5 hours of cooling after the beam operation exceeded 10 mSv/h downstream of ESS1. In order to further increase the intensity of the slow extraction beam, further reducing beam loss in the ESS is necessary. Therefore, we plan to install beam diffusers upstream of the ESS [7]. With beam diffusers, we can scatter particles traveling towards the septum electrode of the ESS at a small angle using multiple Coulomb scattering, thereby reducing the number of particles that collide with the septum electrode. Since the thickness of the septum electrode to be avoided is in the order of tens of micrometer, the scattering angle that needs to be generated by the diffuser is in the order of tens of microradian. This required scattering angle determines the longitudinal length of the diffuser. The cross-section of Coulomb scattering is roughly proportional to Z^2, where Z is the atomic number of the material. The cross-section of the nuclear collision between protons and the nuclei of the material, which causes large-angle scattering leading to beam loss, is roughly proportional to $A^{2/3}$, where A is the mass number of the material. Thus, it is better to choose a material with a large Z as the diffuser and shorten the longitudinal length to reduce the probability of the large angle nuclear scattering in the diffuser. Therefore, we selected tantalum ($A = 181$, $Z = 73$, $\rho = 16.7\,\mathrm{g/cm^3}$) as the material for the diffuser, considering its large Z and good workability.

The J-PARC main ring has two locations where diffusers can be installed. Figure 8 shows those locations. The betatron phase differences between those locations and the ESS are 0.7° and 5°, respectively.

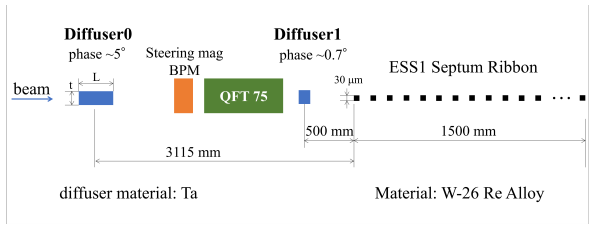

Figure 8: Schematic picture of the diffuser locations at the upstream of the ESS.

We searched for the diffuser sizes in those two locations that maximize the beam loss reduction effect using FLUKA [6]. Table 3 shows the results. Here, the sizes of the diffusers are given in mm, and the beam losses are normalized to the no-diffuser case. The results show that beam losses can be reduced by 65 % by inserting both diffusers. At the position of diffuser 0, where the difference in betatron phase from the ESS is large, the diffuser's longitudinal length can be short. This is because the scattering angle required to avoid the septum electrode of the ESS is small due to the large distance to the ESS. On the other hand, the thickness of the diffuser required to cover the thickness of the septum electrode increases.

Table 3: Optimized Diffuser Lengths, Thicknesses and Corresponding Beam Loss Estimates in Simulation

	Diff0		Diff1		Beam Loss
	t	L	t	L	
No diff	-	-	-	-	1
Diff0 only	0.2	0.5	-	-	0.42
Diff1 only	-	-	0.1	2	0.47
Diff0 & 1	0.2	0.5	0.1	2	0.35

Diffusers of these sizes were installed in the J-PARC Main Ring. Photographs of the installed diffusers are shown in Fig. 9. A beam test was conducted in February 2021. The beam power for the beam test was 10 kW, and only diffuser 0 was inserted. The beam loss distribution in the slow extraction straight section measured by the beam loss monitor is shown in Fig. 10. It can be seen that by inserting diffuser 0, the beam loss was reduced by approximately 60 %, which is consistent with the simulation result.

However, there is one problem. A steering magnet and a BPM that require frequent maintenance are installed immediately downstream of the diffuser 0. Therefore, we are considering swapping the locations of diffuser 0 and these devices. Also, since diffuser 1 is installed directly upstream

ISBN: 978-3-95450-253-0 ISSN: 2673-5571 doi:10.18429/JACoW-HB2023-FRC1I3

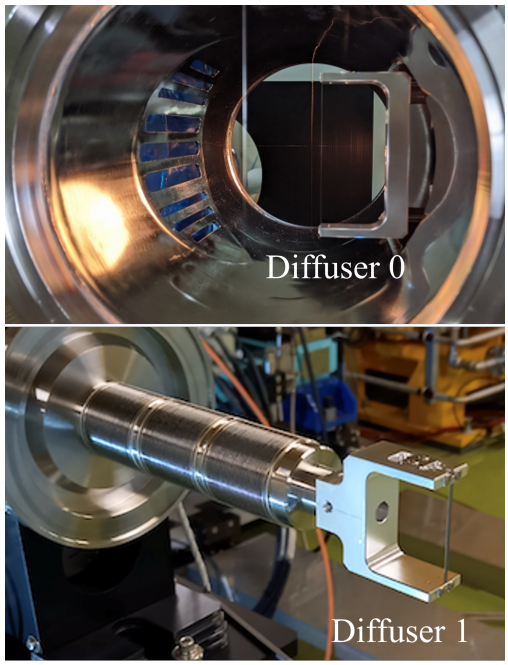

Figure 9: Photos of the two installed diffusers.

of ESS and has no such problem, we are considering using only diffuser 1. We plan to conduct beam tests for both diffuser 0 and diffuser 1 with a high-intensity beam soon.

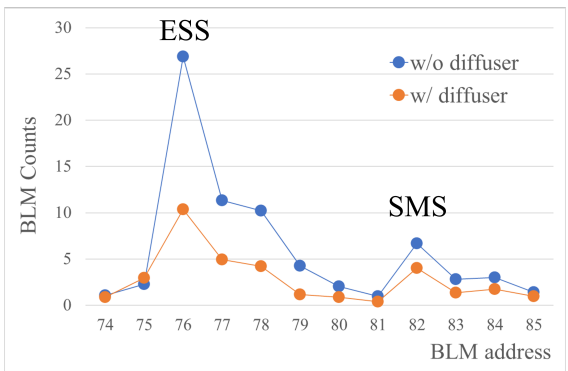

Figure 10: Beam loss distributions with and without the diffuser 0 in the beam test performed with a 10 kW beam.

BEAM COLLIMATOR AT THE DOWNSTREAM OF ESS

Some particles scattered by the septum electrode of the ESS are scattered at large angles and activate devices around the ESS. However, some particles whose scattering angles are not so large are transported downstream, activating downstream devices. In the case of slow extraction of the J-PARC MR, there was a problem that the activation of the Q magnet located 20 m downstream from the ESS became greater than the activation of the ESS itself. Therefore, a beam collimator was installed between the ESS and the Q magnet. As mentioned in the introduction, the J-PARC MR slow extraction straight section has the characteristic that there is sufficient space to install devices between the ESS and the downstream devices. We used MARS [8] to consider the position and size of the collimator. Figure 11 shows the MARS simulation results for the particle fluxes of particles scattered by the

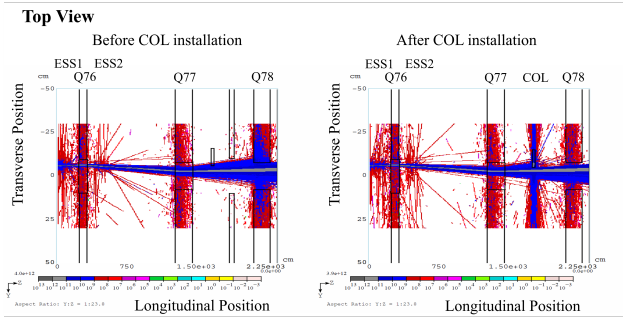

Figure 11: MARS simulation results for fluxes of particles scattered by the ESS. The left panel shows the result without the collimator, and the right panel shows the result with the tungsten collimator downstream of the ESS. In the right panel, it can be seen that the collimator stops the particles from colliding with Q78.

ESS. A cross-sectional view of the tungsten block is shown in Fig. 12. The lengths of the tungsten blocks in the beam axis direction were set to 400 mm to ensure sufficient absorption of 30 GeV protons. The vacuum chamber containing the tungsten block is covered with 10 cm-thick marble blocks, which are characterized by their fairly high radiation shielding effect and their resistance to activation. The vacuum chamber with the marble blocks are covered 30 to 70 cm thick with iron shields. Figure 13 shows a comparison of the

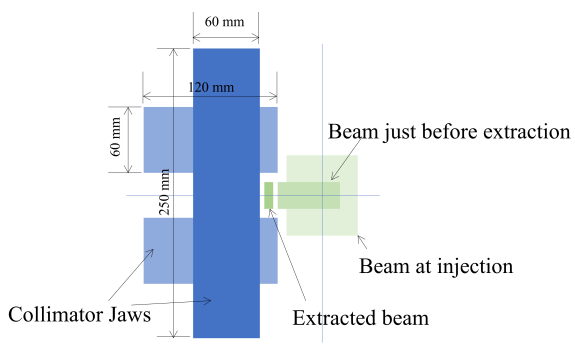

Figure 12: A schematic picture of the cross-section of the collimator viewed from the direction in which a beam enters.

residual dose rate before and after the collimator installation. Measurements were taken after cooling for about 5 hours after operating for about 1 month at a beam power of about 3 kW. It can be seen that the collimator has the expected effect of reducing the residual dose rate of the downstream Q magnet of Q78.

ISBN: 978-3-95450-253-0 ISSN: 2673-5571 doi:10.18429/JACoW-HB2023-FRC1I3

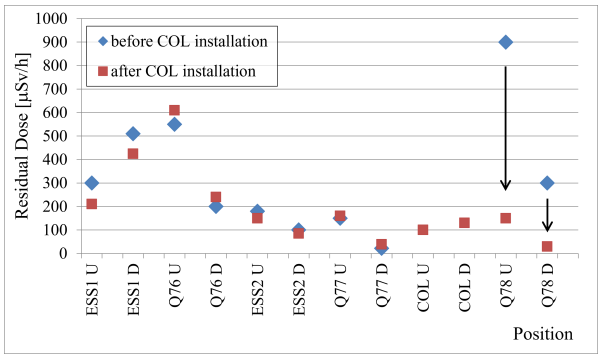

Figure 13: Residual dose rate measurement results for the slow extraction straight section. Blue points show the measurement results before the installation of the collimator, and orange points show those after the installation. The horizontal axis is the measurement position.

FUTURE PLANS

Bent Silicon Crystals for Beam Loss Reduction

Bent silicon crystals are devices that can be expected to have a large beam loss reduction effect. We can make use of its characteristic phenomena such as channeling and volume reflection to deflect the beam and reduce the number of particles that collide with the septum electrode. At the CERN SPS 400 GeV slow extraction beam loss was reduced by about 40 % by introducing the bent silicon crystal [9]. Also for the J-PARC MR slow extraction, a sufficient beam loss reduction effect can be expected with the help of a small angle spread of the proton beam realized by the dynamic bump scheme. We are considering to replace diffuser 0 with a bent silicon crystal in the future.

Search for Low-Z Material for Septum Electrode

The current ESS uses tungsten rhenium alloy as the septum electrode material. This is due to its high tensile strength and high melting point, but the energy deposit in the high-Z material is large. If a septum electrode could be made with low-Z material, the beam loss can be significantly reduced [10]. Carbon nanotubes are one candidate material, but negative test results have already been reported [11]. We plan to conduct high-voltage tests on the carbon nanotubes independently and continue exploring potential materials, including copper-coated carbon nanotubes.

SUMMARY

We developed an electrostatic septa with thin septum electrodes and achieved a high extraction efficiency of about 99.5 % in slow extraction by combining these devices with a dynamic bump scheme in the J-PARC Main Ring. We also installed a beam collimator to suppress the activation of devices downstream of the electrostatic septa, and observed the expected effect. We are planning to carry out the beam test for beam diffusers upstream of the ESS to reduce the number of particles that collide with the septum electrode. In addition, with the aim of further reducing beam losses, we will continue investigating bent silicon crystals, which can be more effective than diffusers, and searching for low-Z materials for septum electrodes.

REFERENCES

[1] Joint Project Team of JAERI and KEK, "The joint project for high-intensity proton accelerators," KEK Report 99–4, Tsukuba, Japan, 1999.

[2] Y. Arakaki *et al.*, "Electrostatic Septum for 50 GeV Proton Synchrotron in J-PARC," in *Proc. IPAC'10*, Kyoto, Japan, May 2010, pp. 3900–3902. http://accelconf.web.cern.ch/IPAC10/papers/THPEB010.pdf

[3] M. Tomizawa *et al.*, "Slow extraction from the J-PARC Main Ring using a dynamic bump," *Nucl. Instrum. Methods Phys. Res., Sect. A*, vol. 902, pp. 51–61, 2018. doi:10.1016/j.nima.2018.06.004

[4] SAD Home Page, https://acc-physics.kek.jp/SAD/.

[5] R. Muto *et al.*, "Manufacturing and operation of the magnetic septa for the slow beam extraction from the J-PARC 50 GeV proton synchrotron," *IEEE Trans. Appl. Supercond.*, vol. 20, no. 3, pp. 336–339, 2010. doi:10.1109/TASC.2010.2040255

[6] C. Ahdida *et al.*, "New capabilities of the FLUKA multi-purpose code," *Front. Phys.*, vol. 9, 2022. doi:10.3389/fphy.2021.788253

[7] R. Muto *et al.*, "Simulation study on double diffuser for loss reduction in slow extraction at J-PARC Main Ring," in *Proc. IPAC'21*, Campinas, Brazil, May 2021, pp. 3069–3072. doi:10.18429/JACoW-IPAC2021-WEPAB192

[8] N. V. Mokhov and S. I. Striganov, "MARS15 overview," *AIP Conf. Proc.*, vol. 896, no. 1, pp. 50–60, 2007. doi:10.1063/1.2720456

[9] F. M. Velotti *et al.*, "Septum shadowing by means of a bent crystal to reduce slow extraction beam loss," *Phys. Rev. Accel. Beams*, vol. 22, p. 093 502, 2019. doi:10.1103/PhysRevAccelBeams.22.093502

[10] M. Tomizawa *et al.*, "Initial tests for electrostatic septum using carbon nanotube wires," *JPS Conf. Proc.*, vol. 33, p. 011 035, 2021. doi:10.7566/JPSCP.33.011035

[11] J. Borburgh, B. Balhan, B. Goddard, L. Jorat, and A. Prost, "Experimental results of low-Z materials as a high voltage septum anode," in *2020 29th International Symposium on Discharges and Electrical Insulation in Vacuum (ISDEIV)*, 2021, pp. 446–449. doi:10.1109/ISDEIV46977.2021.9586893